

# Revised calculation method of concentrations and uncertainties for in-situ CO<sub>2</sub> and CH<sub>4</sub> measurements with a working standard gas saving system

Motoki Sasakawa<sup>1</sup>, Noritsugu Tsuda<sup>2</sup>, Toshinobu Machida<sup>1</sup>, Mikhail Arshinov<sup>3</sup>, Denis Davydov<sup>3</sup>, Aleksandr Fofonov<sup>3</sup>, Boris Belan<sup>3</sup>

<sup>1</sup>Earth Science Division, Center for Global Environmental Research, National Institute for Environmental Studies, Tsukuba, 305-8506, Japan

<sup>2</sup>Global Environmental Forum, Tsukuba, 305-0061, Japan

<sup>3</sup>Institute of Atmospheric Optics, Russian Academy of Sciences, Siberian Branch, Tomsk, Russia

Correspondence to: Motoki Sasakawa (sasakawa.motoki@nies.go.jp)

**Abstract.** We have revised a calculation method of concentrations and uncertainties for in-situ CO<sub>2</sub> and CH<sub>4</sub> measurements with a working standard gas saving system. It uses on-site compressed air to track the baseline drift of sensors. JR-STATION (Japan-Russia Siberian Tall Tower Inland Observation Network) was made up of this system, which was installed across nine different sites in Siberia. The system acquires semi-continuous data by recording several minutes of averaged data after gas replacement time. We have updated the calculation method for deriving CO<sub>2</sub> and CH<sub>4</sub> concentrations to determine their uncertainty for each data simultaneously. Furthermore, we estimated the system's reproducibility in about one week based on the repeated measurement of on-site compressed air. The CO<sub>2</sub> and CH<sub>4</sub> concentration reproducibility mostly varied by less than 0.2 ppm and five ppb, respectively. Uncertainties of time-averaged data were sometimes higher than the measurement uncertainty (reproducibility) for each period because the data include atmospheric variability during the measurement period of several minutes. Data users should consider the difference between the two uncertainties to select optimal data, depending on their focusing spatial scale. The CO<sub>2</sub> and CH<sub>4</sub> data measured with the NDIR and the tin dioxide sensor exhibited good agreement with those measured by the CRDS.

## 1 Introduction

It is known that accurate measurements of greenhouse gas concentrations require the analyzers to be calibrated against a set of standard gas mixtures. At least one of them (target) should be used hourly to track an NDIR (Non-Dispersive Infrared) analyzer's baseline drift (Andrews et al., 2014). Delivering high-pressure cylinders to remote sites is a significant issue for long-term atmospheric monitoring. Thus, to reduce the consumption of gas, Watai et al. (2010) developed a system that utilizes on-site air as sub-working standard gas (SWS-gas) to track the baseline drift of the NDIR sensors. Watai et al. (2010) then installed this system at a remote tower site at Berezhnezhka (56°08'45"N 84°19'55"E) in West Siberia in 2001 to measure CO<sub>2</sub> concentrations semi-continuously. After this, in Central Siberia, Winderlich et al. (2010) developed a measuring system

削除: Working standard gas saving system for in-situ CO<sub>2</sub> and CH<sub>4</sub> measurements and

削除: for

削除: their

削除: y

削除: develop

削除: container system for in-situ measurement

削除: that

削除: significantly reduces the consumption of

削除:

削除: es

削除: to a level less than one order of magnitude smaller than that required by a common method.

削除: consisted

削除: t

削除: ,

削除: suggesting that

削除: , respectively

削除: A CRDS (Cavity Ring-Down Spectroscopy) analyzer is more stable and does not need frequent checks of the drift (ICOS RI, 2020). ...

without dehumidification using a CRDS (Cavity Ring-Down Spectroscopy) analyzer, an ingenious way to reduce the frequency of cylinder replacement. The CRDS is a more stable device, and a calibration frequency of every two weeks to every month is recommended (ICOS RI, 2020).

55 Concerning CH<sub>4</sub> measurement, a commonly used gas chromatograph with a flame ionization detector (GC/FID) requires hydrogen and carrier gases. It also needs significant power consumption. However, electric power is often restricted at remote sites. Thus, Suto and Inoue (2010) modified a tin dioxide sensor (TOS), which is widely used to detect natural gas leaks, to be able to measure CH<sub>4</sub> in the atmosphere. The developed TOS unit does not need hydrogen and carrier gases. The nominal power consumption for the unit, consisting of TOS, temperature-stabilizer mechanism, and electronic circuits for the sensor and  
60 heater, is less than 10W.

We added the TOS unit to the system at the tower site in West Siberia, then expanded the tower observation network (Sasakawa et al., 2010; Sasakawa et al., 2012; Sasakawa et al., 2013). The tower network named JR-STATION (Japan-Russia Siberian Tall Tower Inland Observation Network) now consists of six tower sites in West Siberia. Recently, we added CRDS analyzers at Karasevov (58°14'44"N 82°25'28"E) in 2015 (Picarro G2401), and at Demyanskoe (59°47'29"N 70°52'16"E) and Noyabrsk  
65 (63°25'45"N 75°46'48"E) in 2016 (Picarro G2301) to improve the robustness of the measurements. We have further updated the calculation method for calculating CO<sub>2</sub> and CH<sub>4</sub> concentrations to derive their uncertainty for each data simultaneously. Here, we describe the details of the modified measurement system and the calculation method. We also compare the data produced with the NDIR (and the semiconductor sensor) and the CRDS data.

## 2 Method

### 70 2.1 Measurement system

Ambient air was taken from air sample inlets at two different heights (four at Berezhovka) on television and radio-relay communication towers (Table 1). Each sample inlet was mounted several meters away from the tower at the end of an extension arm. The air from the inlets was pulled into the measurement system through the sampling lines (6-mm OD Decabon tube).  
The measurement system was housed in a freight container insulated to reduce temperature variation. Two thermometers were  
75 mounted inside the container, one near the ceiling and the other near the floor. According to the upper thermometer, the room temperature in the container during the year was kept above 15°C and the temperature difference in the 12-hour calibration interval was kept below 3°C on average during the year. Since the introduction of the CRDS, a simple cooler was installed to prevent the temperature inside the container from rising too high during the summer months due to the heat generated by the CRDS. A schematic diagram of the measurement system is shown in Fig. 1. The measurement system consists of a pump unit,  
80 a selector unit, and an analyzer unit. The pump unit was located upstream of the selector and analyzer unit to keep the downstream pressure higher than the ambient, which reduced the likelihood of bias in measurements due to any leak from many connections in the system. Two diaphragm pumps (model N86KNE, KNF, Germany) delivered the sample air into the system. The sampling lines were flushed continuously with a flow rate of about seven standard liters per minute, and excess

删除: suck

85 air was vented through the back-pressure valve ("BPV" in the pump unit). Then the air was dried by an adiabatic expansion in  
a glass water trap ("WT" in the pump unit) that was purged every hour via an NC solenoid valve, which was opened twice for  
10 seconds to remove the condensed water. The sample air was also dried using a semipermeable membrane dryer (PD-625–  
24SS, Permapure, USA) ("Nafion" in the selector unit) in the selector unit. The semipermeable membrane dryer removed water  
vapor from the pressurized inner tube to an outer tube where the split gas flowed (split sample method). The air from the upper  
90 and lower-level inlet, the three working standard gases (WS-gases), and the sub-working standard gas (SWS-gas) were  
selected through a 6-port valve manifold. While the WS-gases or the SWS-gas flowed into the analyzer unit, the sample air  
was exhausted at the 6-port valve. In the analyzer unit, the sampled air was extra dried with magnesium perchlorate, which  
was fed into a stainless steel tube with a dimension of 2 cm in inner diameter and 10 cm in length ("Mg(ClO<sub>4</sub>)<sub>2</sub>" in the analyzer  
unit). There were two tubes, and the flow path of the air switched from one to the other every month. The used magnesium  
95 perchlorate was replaced before the next run. After being dried with the magnesium perchlorate, the air retained its dewpoint  
at around -50 °C (39 ppm). The dehumidified air was then introduced into an NDIR analyzer (LI-820, LI-COR, USA; LI-7000  
was used until September 2008 at BRZ) at a constant flow rate of 35 standard cubic centimeters per minute (sccm) set by a  
mass flow controller (SEC-E40, STEC, Japan). The CO<sub>2</sub> concentration was defined as the mole fraction in the dry air, and  
water vapor correction was not adopted. After passing through the NDIR, the air flowed into the TOS unit. A chemical  
100 desiccant made of P<sub>2</sub>O<sub>5</sub> was installed in front of the TOS because it is necessary to keep water vapor below ten ppm in the  
sample air for this type of sensor. The sensor was designed to operate in areas lacking the sufficient infrastructure to sustain a  
conventional measurement system, such as a significant power source, carrier gas supply, and temperature-stabilized  
environment. The sensor has been verified against a gas chromatograph equipped with a flame ionization detector (Suto and  
Inoue, 2010). We additionally installed the CRDS (Picarro Inc.) analyzer at Karasevov (G2401) in 2015, and at Demyanskoe  
105 and Noyabrsk (G2301) in 2016 to improve the system. The sampled air was split after leaving the 6-port valve, then fed into  
the CRDS at a constant flow rate of 35 sccm set by a mass flow controller (SEC-E40, STEC, Japan) through a semipermeable  
membrane dryer (model MD-050-72S-1, Permapure, USA). To protect the cavity of the CRDS from an inflow of the dissolved  
chemical desiccant (Mg(ClO<sub>4</sub>)<sub>2</sub> or P<sub>2</sub>O<sub>5</sub>) in the accidental case of a broken pump etc., we equipped the CRDS with two poppet  
check valves ("PCV" in the analyzer unit). When the pumps in the pump unit stop and only the CRDS pump is running, the  
110 flow stops at the PCV upstream of P<sub>2</sub>O<sub>5</sub>, and the increased suction pressure allows air in the container to enter from the PCV  
in front of Nafion. The data from this process has been deleted.  
Three WS-gases (STD1, STD2, STD3) were prepared from pure CO<sub>2</sub> and CH<sub>4</sub> (G1 grade, Japan Fine Products Corp. (JFP),  
Japan) diluted with purified air (G1 grade, JFP), and their concentrations were determined against the NIES 09 CO<sub>2</sub> scale  
(Machida et al., 2011) and NIES 94 CH<sub>4</sub> scale. Each scale was established by a series of standard gases prepared by the  
115 gravimetric method. Since the pure CO<sub>2</sub> gas is derived from burned petroleum, the isotopic CO<sub>2</sub> composition of the es gases  
shows lighter than atmospheric CO<sub>2</sub>. When the NDIR analyzer is calibrated against CO<sub>2</sub> standards with lighter-than-  
atmospheric CO<sub>2</sub> isotopic composition, the NDIR analyzer measures a lower CO<sub>2</sub> mole fraction in a sample air with known  
CO<sub>2</sub> concentration. The error in the apparent NDIR CO<sub>2</sub> mole fraction depends on its individual sensitivity to the optical filter

削除: working standard

書式を変更: 下付き

書式を変更: 下付き

書式を変更: 上付き/下付き(なし)

削除: working standard

書式を変更: 下付き

書式を変更: 下付き

書式を変更: 下付き

書式を変更: 下付き

書式を変更: 下付き

property. Tohjima et al. (2009) reported that the errors for the three NDIR analyzers range from -0.04 to -0.08 ppm. The CO<sub>2</sub> values measured by the system may appear low in the range of up to 0.08 ppm. Compared to the WMO-CO<sub>2</sub>-X2007 scale, the NIES 09 CO<sub>2</sub> scale is consistent within 0.1 ppm (Round Robin 5 and 6 Comparison Experiment). The NIES 94 CH<sub>4</sub> scale ranges from 3.0 to 5.5 ppb higher than the WMO-CH<sub>4</sub>-X2004A scale (Round Robin 5 and 6 Comparison Experiment).

Table 1. Main features of the towers in the network of tall towers used for continuous long-term atmospheric CO<sub>2</sub> and CH<sub>4</sub> measurements over Siberia.

| Identifying Code | Location     | Latitude  | Longitude  | Air inlet heights (m) | Elevation at tower base (m a.s.l) <sup>1</sup> |
|------------------|--------------|-----------|------------|-----------------------|--|
| BRZ              | Berezorechka | 56°08'45" | 84°19'55"  | 5, 20, 40, 80         | 168  |
| KRS              | Karasevoe    | 58°14'44" | 82°25'28"  | 35, 67                | 76   |
| IGR              | Igrim        | 63°11'30" | 64°24'50"  | 24, 47                | 9  |
| NOY              | Noyabrsk     | 63°25'45" | 75°46'48"  | 21, 43                | 108  |
| DEM              | Demyanskoe   | 59°47'29" | 70°52'16"  | 45, 63                | 63   |
| SVV              | Savvushka    | 51°19'31" | 82°07'42"  | 27, 52                | 495  |
| AZV              | Azovo        | 54°42'18" | 73°01'45"  | 29, 50                | 110  |
| VGN              | Vaganovo     | 54°29'50" | 62°19'29"  | 42, 85                | 192  |
| YAK              | Yakutsk      | 62°05'19" | 129°21'21" | 11, 77                | 264  |

<sup>1</sup>Approximate estimates from Google earth.

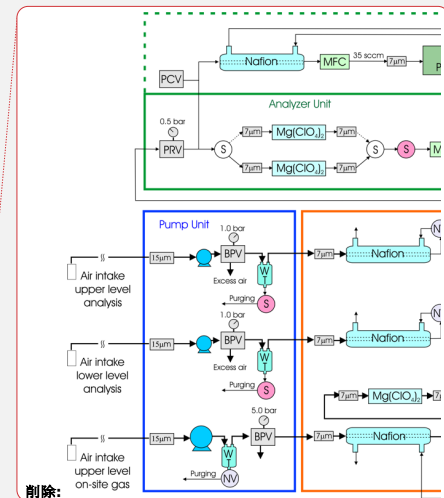
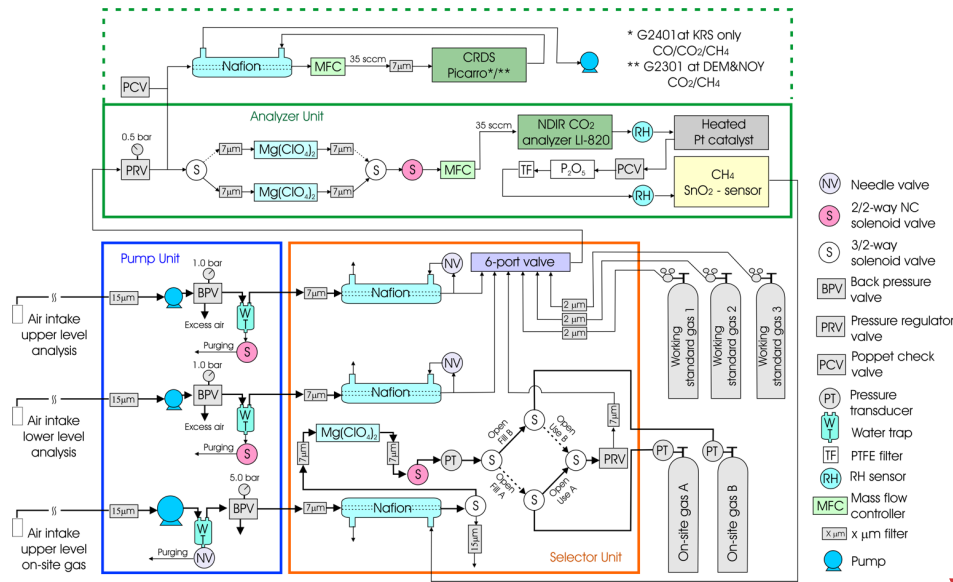
書式を変更: 下付き

削除: 09

削除: lower at a concentration of 376.2 ppm and 0.04 ppm lower at 404.91 ppm ...

削除: is 4.1

削除: at a concentration of 1736.3 ppb and 5.5 ppb higher at 1941.9 ppb ...



削除:

削除: working standard

書式変更: インデント: 最初の行: 1 字

削除: working standar

削除: d

削除:

削除: working standard

削除:

書式を変更: 上付き

削除: To prepare the SWS-gas, air from the highest inlet was compressed by a pump (LOA-P103-NO, GAST, USA) into an aluminum cylinder (0.048 m<sup>3</sup>) for about 5 hours to approximately 0.35 MPa, after having been passed through a similar triple dehumidification path as the sampled air (a stainless steel water trap, a semipermeable membrane dryer (SWF- M06-400, AGC, Japan), and magnesium perchlorate). Two cylinders were prepared for the SWS-gas; one for compression and preservation and the other for the hourly measurements. The cylinders were automatically exchanged when the inner pressure in one used for measurements decreased below 0.1 MPa, which generally took about one week.

is smaller if larger cylinders are used. Given the cylinder size and filling pressure in this system, concentration changes within the cylinder are considered negligible. The variations in SWS concentration with CRDS between WS-gases (48 hours) were in fact very stable regardless of the SWS concentration range (Fig. S1-2). Air temperature and relative humidity were measured at both heights on the tower using commercial sensors (HMP45D, Vaisala, Finland). A wind monitor (model 81000, R. M. Young, USA) determined wind direction and speed at the higher inlet. Solar radiation was measured by a pyranometer (CM3, Kipp & Zonen, Netherlands), and precipitation by a tipping bucket rain gauge (model 52202, R. M. Young, USA) on the top of the container laboratory.

The analysis operation and data logging were performed by a measurement and control system (CR10X datalogger, CAMPBELL, USA). Stored data were retrieved once a month when both a system check and replacement of consumables (e.g., chemical desiccants) took place.

删除:

## 2.2 Measurement sequence

To be able to measure air at two heights, the air-sampling flow path was rotated every 20 min with the 6-port valve in the selector unit; that is, the higher inlet was sampled from hh:00 to hh:20, the lower inlet from hh:20 to hh:40, and the SWS-gas from hh:40 to (hh+1):00. During the first 17 min of each 20-min sampling interval, the system is flushing to equilibrate the air sample after switching. The final three-minute readouts were averaged and reported as the representative output data for the applicable one-hour period. Measurement frequency was 3 sec; thus, only the average and standard deviation of 60 readouts in voltage were stored in the CR10X. This was to minimize the data size for the limited storage capacity. The timestamp was the end time of every 20-min measurement interval. The raw data collected with the CRDS analyzer were stored in the CRDS' hard disk and processed after downloading in our laboratory.

Figure 2 shows the schematic measurement sequence for half a day. In the Fig. 2, we defined when the SWS-gas was measured just before an arbitrary series of WS-gas measurements as  $t_0$ . Then we numbered the time of the following measurements in turn. We also defined the series of standard gas measurements at the beginning of the 12 hours as “B” and at the end as “E”.

删除: To exclude unreliable data, sometimes resulting from the system malfunction, the data was not used for sample calculation when the average data for the SWS-gas or working standard gases, which show essentially slight fluctuation, had a more significant standard deviation than a determined threshold (2 mV for CO<sub>2</sub>, 5 mV for CH<sub>4</sub>). Furthermore, we did not calculate the concentration of the sample when the outputs of the adjacent SWS-gas measurements varied largely.

删除: working standard

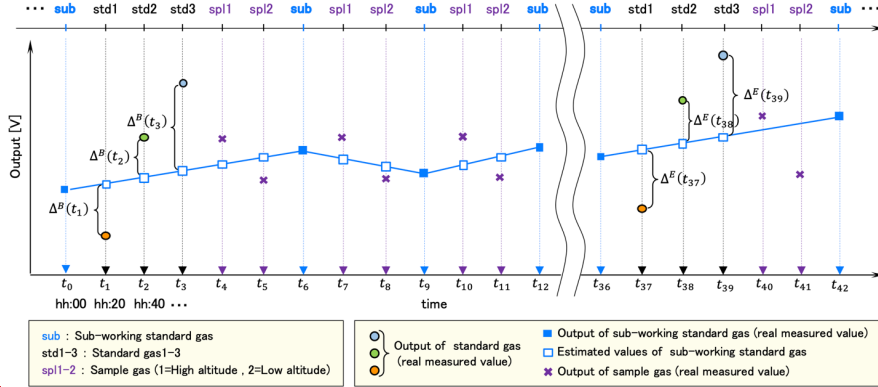


Figure 2. Measurement sequence for a half day between subsequent measurements of WS-gases.

### 2.3 Quality check of the standard gas measurements

First, we checked the relationship among three standard gas measurements. We calculated the differences ( $\Delta^B(t_i)$ ,  $\Delta^E(t_j)$ ) between the measured output voltages of the standard gases ( $V_{std}(t_i)$ ,  $V_{std}(t_j)$ ) and the estimated one of the SWS-gas at the time of the standard gas measurement (Fig. 2). Here  $i = 1, 2, 3$ , and  $j = 37, 38, 39$ . The output value of the SWS-gas was interpolated by time using the closest output of the SWS-gas before and after the series of standard gas measurements. Thus, these values and their variances are expressed as:

$$\Delta^B(t_i) = V_{std}(t_i) - \left( \frac{6-i}{6} \cdot V_{sub}(t_0) + \frac{i}{6} \cdot V_{sub}(t_6) \right) \quad (1)$$

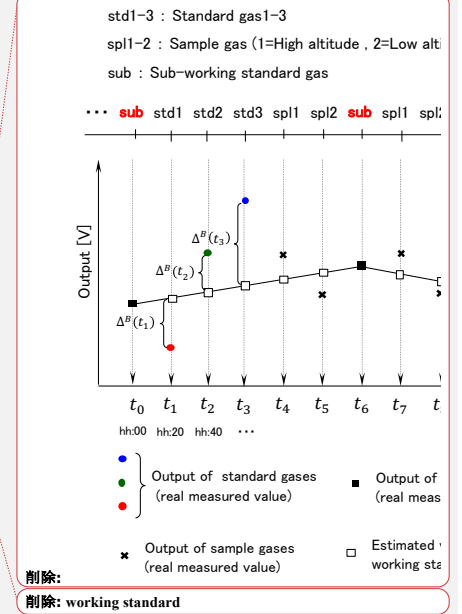
$$(\sigma^B(t_i))^2 = (\sigma_{std}(t_i))^2 + \left( \frac{6-i}{6} \cdot \sigma_{sub}(t_0) \right)^2 + \left( \frac{i}{6} \cdot \sigma_{sub}(t_6) \right)^2 \quad (2)$$

$$\Delta^E(t_j) = V_{std}(t_j) - \left( \frac{42-j}{6} \cdot V_{sub}(t_{36}) + \frac{j-36}{6} \cdot V_{sub}(t_{42}) \right) \quad (3)$$

$$(\sigma^E(t_j))^2 = (\sigma_{std}(t_j))^2 + \left( \frac{42-j}{6} \cdot \sigma_{sub}(t_{36}) \right)^2 + \left( \frac{j-36}{6} \cdot \sigma_{sub}(t_{42}) \right)^2 \quad (4)$$

We estimated the output of STD1 at  $t_2$  by adding  $\Delta^B(t_1)$  to the estimated one of the SWS-gas at  $t_2$ . We also evaluated the output of STD3 at  $t_2$  by adding  $\Delta^E(t_3)$  to the estimated one of the SWS-gas at  $t_2$ . The same estimation was done at  $t_{38}$ . We then made a linear calibration line with the output of STD2 and the estimated outputs of STD1 and STD3. Only those sets of the three standard gas measurements whose coefficients of determination were higher than 0.999 for CO<sub>2</sub> and 0.99 for CH<sub>4</sub> were adopted for the following calculation.

The difference in output (voltage) between  $\Delta^B$  and  $\Delta^E$  for each standard gas was defined as follows:



$$\delta_{(1,37)} = \Delta^E(t_1) - \Delta^B(t_{37}) \quad (5)$$

$$\delta_{(2,38)} = \Delta^E(t_2) - \Delta^B(t_{38}) \quad (6)$$

$$\delta_{(3,39)} = \Delta^E(t_3) - \Delta^B(t_{39}) \quad (7)$$

230 The  $\delta$  must be small unless the system is unstable, e.g., when the sensitivity of the sensors changes considerably for some reason. To exclude the data obtained during system malfunction, we determined a threshold for  $\delta$  by converting it into concentration (<5.0 ppm for CO<sub>2</sub>, <50 ppb for CH<sub>4</sub>). Data showing values over the threshold were excluded from the calculation. The difference in CO<sub>2</sub> concentration between sides *B* and *E* was calculated as follows:

$$\overline{\delta_{(i,j)}^B} = |\delta_{(i,j)} / S^B| \quad (8)$$

$$\overline{\delta_{(i,j)}^E} = |\delta_{(i,j)} / S^E| \quad (9)$$

235 where  $S^B$  and  $S^E$  are the slopes of the linear regression line at sides *B* and *E*. Because the x-axis of the calibration line for CH<sub>4</sub> is the logarithm of the concentration, the difference in CH<sub>4</sub> concentrations was calculated as:

$$\overline{\delta_{(i,j)}^B} = C_i \cdot \left| e^{\frac{\delta_{(i,j)}}{S^B}} - 1 \right| \quad (10)$$

$$\overline{\delta_{(i,j)}^E} = C_i \cdot \left| e^{-\frac{\delta_{(i,j)}}{S^E}} - 1 \right| \quad (11)$$

where  $C_i$  is the concentration of the standard gas.

240

#### 2.4 Calculation of the sample concentration and its uncertainty

245 The analysis precision for this system under laboratory conditions was uniformly estimated as 0.3 ppm for CO<sub>2</sub> (Watai et al., 2010). Concerning CH<sub>4</sub> precision, Sasakawa et al. (2010) estimated it as 3.0 ppb based on the result of Suto and Inoue (2010). However, the experiment condition by Suto and Inoue (2010) was different from the gas-saving system. Instead, they connected only the WS-gases to the TOS, then reported the standard deviation of repeated measurements. The CH<sub>4</sub> analysis precision for this system thus could be more significant than 3.0 ppb. Furthermore, the sensitivity and stability of the sensor could differ depending on the individual sensor and the condition of the individual system. We thus have updated the method for calculating the CO<sub>2</sub> and CH<sub>4</sub> concentrations to derive their uncertainty for each data simultaneously.

削除: working standard

##### 250 2.4.1 Estimation of the output values of working standard gases and their uncertainty at the time of the air sample measurements

We estimated the outputs in voltage of three standard gases at each measurement time of the sample air by interpolating the outputs of the three WS-gases depending on the difference of the outputs in voltage of the SWS-gas only when both standard gas measurements satisfied the criteria described in section 2.3. Depending on the time difference between the targeted sample

削除: working standard

削除: between

削除: es



( $t_k; k = 4, 5, 7, 8, \dots, 34, 35$ ) and standard gases at both sides  $B$  and  $E$  ( $((t_i, t_j); (i, j) = (1, 37), (2, 38), (3, 39))$ ), the representative value ( $\hat{V}_{std(t_i, t_j)}^{BE}(t_k)$ ) and its variance ( $(\sigma_{std(t_i, t_j)}^{BE}(t_k))^2$ ) were estimated as follows (Fig. 3):

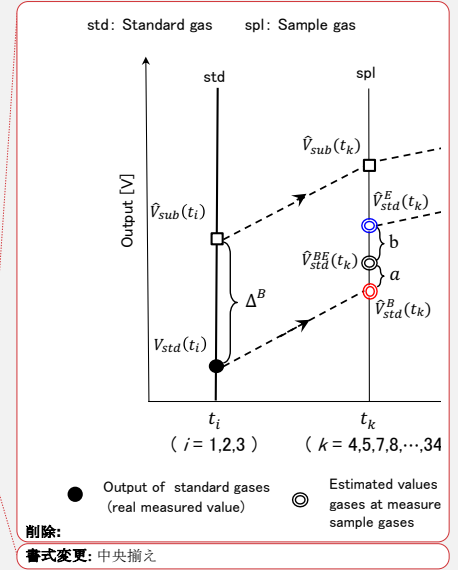
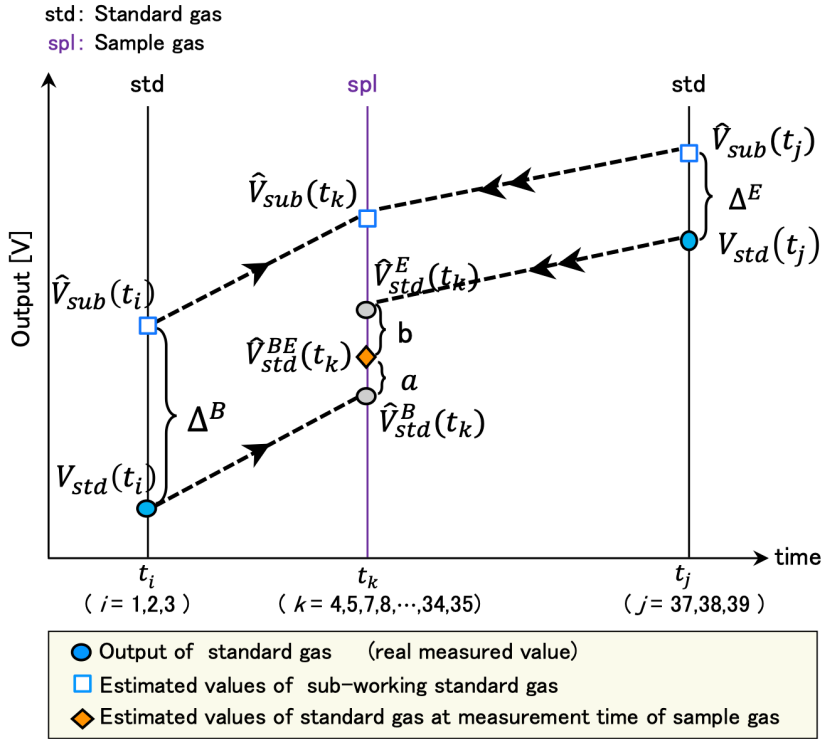


Figure 3. Schematic diagram of the estimation method for the output of the standard gas at the time of sample air measurement.

$$\begin{aligned}
 \hat{V}_{std(t_i, t_j)}^{BE}(t_k) &= \frac{a}{a+b} \cdot \hat{V}_{std(t_i)}^B(t_k) + \frac{b}{a+b} \cdot \hat{V}_{std(t_j)}^E(t_k) \\
 &= \hat{V}_{sub}(t_k) + \frac{1}{a+b} \cdot \{ a \cdot \Delta^B(t_i) + b \cdot \Delta^E(t_j) \} \\
 (\sigma_{std(t_i, t_j)}^{BE}(t_k))^2 &= (\sigma_{sub}(t_k))^2 + \left( \frac{a}{a+b} \cdot \sigma_{std(t_i)} \right)^2 + \left( \frac{a}{a+b} \cdot \frac{6-i}{6} \cdot \sigma_{sub}(t_0) \right)^2
 \end{aligned} \tag{12}$$

$$\begin{aligned}
& + \left( \frac{a}{a+b} \cdot \frac{i}{6} \cdot \sigma_{sub}(t_6) \right)^2 + \left( \frac{b}{a+b} \cdot \sigma_{std}(t_j) \right)^2 + \left( \frac{b}{a+b} \cdot \frac{42-j}{6} \cdot \sigma_{sub}(t_{36}) \right)^2 \\
& + \left( \frac{b}{a+b} \cdot \frac{j-36}{6} \cdot \sigma_{sub}(t_{42}) \right)^2
\end{aligned} \tag{13}$$

270 where  $a : b = (t_j - t_k) : (t_k - t_i)$ . Hat “^” means estimated value.  $V_{sub}(t_k)$  was calculated by interpolating the output of the SWS-gas value nearest to the targeted sample as follows:

$$\begin{aligned}
& \{spl1 \mid k = 4\} \\
& V_{sub}(t_4) = \frac{1}{3} \cdot V_{sub}(t_0) + \frac{2}{3} \cdot V_{sub}(t_6)
\end{aligned} \tag{14}$$

$$\begin{aligned}
& \{spl1 \mid k = 7, 10, 13, \dots, 34\} \\
275 \quad V_{sub}(t_k) = \frac{2}{3} \cdot V_{sub}(t_{k-1}) + \frac{1}{3} \cdot V_{sub}(t_{k+2})
\end{aligned} \tag{15}$$

$$\begin{aligned}
& \{spl2 \mid k = 5\} \\
& V_{sub}(t_5) = \frac{1}{6} \cdot V_{sub}(t_0) + \frac{5}{6} \cdot V_{sub}(t_6)
\end{aligned} \tag{16}$$

$$\begin{aligned}
& \{spl2 \mid k = 8, 11, 14, \dots, 35\} \\
& V_{sub}(t_k) = \frac{1}{3} \cdot V_{sub}(t_{k-2}) + \frac{2}{3} \cdot V_{sub}(t_{k+1})
\end{aligned} \tag{17}$$

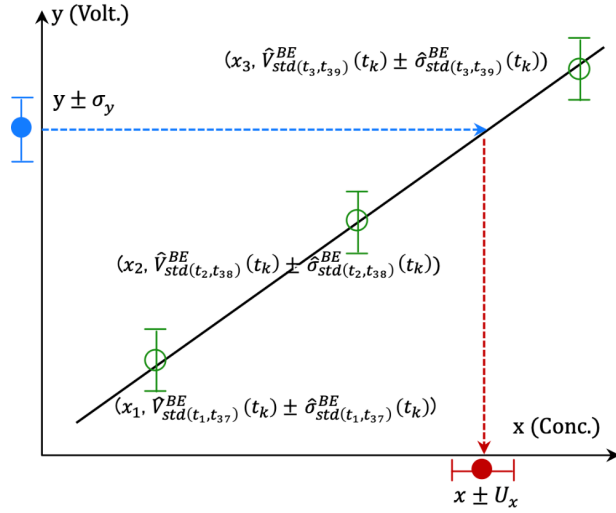
280 Here  $V_{sub}(t_l) \{sub \mid l = 0, 6, 9, 12, \dots, 36\}$  is the measured value. In the following, a calculation example of  $V_{std(t_i, t_j)}^{BE}$  and the variance for the case  $\{spl1 \mid k = 4, (i, j) = (1, 37), (2, 38), (3, 39)\}$  are given without any estimated value.

$$\begin{aligned}
& \{spl1 \mid k = 4, (i, j) = (1, 37), (2, 38), (3, 39)\} \\
& V_{std(t_i, t_j)}^{BE}(t_4) = \frac{1}{3} \cdot V_{sub}(t_0) + \frac{2}{3} \cdot V_{sub}(t_6) + \frac{a}{a+b} \cdot \left\{ V_{std}(t_i) - \left( \frac{6-i}{6} \cdot V_{sub}(t_0) + \frac{i}{6} \cdot V_{sub}(t_6) \right) \right\} \\
& + \frac{b}{a+b} \cdot \left\{ V_{std}(t_j) - \left( \frac{42-j}{6} \cdot V_{sub}(t_{36}) + \frac{j-36}{6} \cdot V_{sub}(t_{42}) \right) \right\}
\end{aligned} \tag{18}$$

$$\begin{aligned}
285 \quad & \left( \sigma_{std(t_i, t_j)}^{BE}(t_4) \right)^2 = \left( \frac{1}{3} \cdot \sigma_{sub}(t_0) \right)^2 + \left( \frac{2}{3} \cdot \sigma_{sub}(t_6) \right)^2 \\
& + \left( \frac{a}{a+b} \cdot \sigma_{std}(t_i) \right)^2 + \left( \frac{a}{a+b} \cdot \frac{6-i}{6} \cdot \sigma_{sub}(t_0) \right)^2 + \left( \frac{a}{a+b} \cdot \frac{i}{6} \cdot \sigma_{sub}(t_6) \right)^2 \\
& + \left( \frac{b}{a+b} \cdot \sigma_{std}(t_j) \right)^2 + \left( \frac{b}{a+b} \cdot \frac{42-j}{6} \cdot \sigma_{sub}(t_{36}) \right)^2 + \left( \frac{b}{a+b} \cdot \frac{j-36}{6} \cdot \sigma_{sub}(t_{42}) \right)^2
\end{aligned} \tag{19}$$

### 2.4.2 Estimation of sample air concentration and estimation uncertainty using a calibration line

290 We calculated a calibration line with the estimated outputs of standard gases ( $\hat{V}_{std(t_i, t_j)}^{BE}(t_k)$ ) and their variances ( $(\hat{\sigma}_{std(t_i, t_j)}^{BE}(t_k))^2$ ) at the time of the sample measurement obtained in the section 2.4.1. A linear line ( $y = Sx + I$ ;  $y$ : output in voltage,  $x$ : concentration for CO<sub>2</sub> and log(concentration) for CH<sub>4</sub>) was adopted for the calibration line (Fig. 4).



書式変更: 中央揃え

Figure 4. Schematic diagram for estimating the CO<sub>2</sub> and CH<sub>4</sub> concentration ( $x$ ) of the gases and estimation uncertainty ( $U_x$ ) from the output in voltage ( $y$ ) with its standard deviation ( $\sigma_y$ ). The gray line indicates the estimated linear calibration line ( $y = Sx + I$ ).

Following the likelihood method, we identified the slope ( $S$ ) and intercept ( $I$ ) for every sample time ( $k$ ) at the maximum of the

likelihood function ( $L$ ). Solving the normal equation of  $\begin{cases} \frac{\partial L}{\partial S} = 0 \\ \frac{\partial L}{\partial I} = 0 \end{cases}$ ,  $S$  and  $I$  were obtained as follows:

$$S(k) = \frac{(\sum w_{ijk})(\sum w_{ijk}x_i y_{ijk}) - (\sum w_{ijk}x_i)(\sum w_{ijk}y_{ijk})}{(\sum w_{ijk})(\sum w_{ijk}x_i^2) - (\sum w_{ijk}x_i)^2} \quad (20)$$

$$300 \quad I(k) = \frac{(\sum w_{ijk}y_{ijk})(\sum w_{ijk}x_i^2) - (\sum w_{ijk}x_i y_{ijk})(\sum w_{ijk}x_i)}{(\sum w_{ijk})(\sum w_{ijk}x_i^2) - (\sum w_{ijk}x_i)^2} \quad (21)$$

削除:

改ページ

<オブジェクト>

①  
 ②  
 ③  
 ④  
 ⑤  
 ⑥  
 ⑦  
 ⑧  
 ⑨  
 ⑩  
 ⑪  
 ⑫  
 ⑬  
 ⑭  
 ⑮  
 ⑯  
 ⑰  
 ⑱  
 ⑲  
 ⑳  
 ㉑  
 ㉒  
 ㉓  
 ㉔  
 ㉕  
 ㉖  
 ㉗  
 ㉘  
 ㉙  
 ㉚  
 ㉛  
 ㉜  
 ㉝  
 ㉞  
 ㉟  
 ㊱  
 ㊲  
 ㊳  
 ㊴  
 ㊵  
 ㊶  
 ㊷  
 ㊸  
 ㊹  
 ㊺  
 ㊻  
 ㊼  
 ㊽  
 ㊾  
 ㊿

削除: working standard

where  $x_i$  is WS-gas concentration determined against the NIES scale.  $y_{ijk}$  is the estimated outputs of standard gas

$(V_{std(t_i, t_j)}^{BE}(t_k))$  and  $w_{ijk}$  is the reciprocal of the variance  $(1/\left(\sigma_{std(t_i, t_j)}^{BE}(t_k)\right)^2)$ .  $\Sigma$  indicates the sum of  $i$  (three standard gases)

320 and the same for the following discussion. As shown in Section 2.4.1, the combinations of (i, j) are (1, 37), (2, 38), and (3, 39).

We omitted  $i$ ,  $j$ , and  $k$  for the following expression. The inverse function was used because we estimated the concentration from the output in voltage. Furthermore, because the calibration line passes through the weighted mean point  $(x, y) =$

$(\frac{\sum wx}{\sum w}, \frac{\sum wy}{\sum w})$ , we practically used the following line:

$$x = \frac{y - \bar{y}}{s} + \bar{x} \quad (22)$$

325 The uncertainty for the estimated concentration ( $x$ ) was calculated with the following equation:

$$U_x^2 = \left(\frac{\partial x}{\partial y}\right)^2 U^2(y) + \left(\frac{\partial x}{\partial y}\right)^2 U^2(y) + \left(\frac{\partial x}{\partial s}\right)^2 U^2(s) + \left(\frac{\partial x}{\partial x}\right)^2 U^2(x) \quad (23-1)$$

where  $U$  is uncertainty for each component. The first term expresses the contribution from the variation in output of the measured air ( $\sigma_y$ ) and 60 repeated measurements:

$$\left(\frac{\partial x}{\partial y}\right)^2 U^2(y) = \frac{\sigma_y^2}{s^2} \cdot \frac{1}{60}$$

330 The second term expresses the contribution from the variation in  $y$ :

$$\left(\frac{\partial x}{\partial y}\right)^2 U^2(y) = \frac{1}{s^2} \cdot \frac{\sum w^2 \sigma^2}{(\sum w)^2} = \frac{1}{s^2} \cdot \frac{1}{\sum w}$$

where  $\sigma^2$  is the variance of the output for standard gases constituting the calibration line. The third term expresses the contribution from the variation in the slope of the calibration line ( $S$ ):

$$\left(\frac{\partial x}{\partial s}\right)^2 U^2(s) = \frac{(y - \frac{\sum wy}{\sum w})^2}{s^4} \cdot \sum \sigma^2 \left(\frac{\partial s}{\partial y}\right)^2 = \frac{(y - \frac{\sum wy}{\sum w})^2}{s^4} \cdot \frac{\sum w}{(\sum w)(\sum wx^2) - (\sum wx)^2}$$

335 The fourth term expresses the contribution from the variation in  $x$ . The NIES09 scale is based on the gravimetric primary standard gases using a one-step dilution (Tohjima et al., 2006), and its overall uncertainty, including transfer, is estimated to be 0.043 ppm (Machida et al., 2011). This value is equal to  $U(x)$ , but this term is not included in the calculation because  $U(x)$  cannot be determined precisely; as for the value of  $U(x)$ , it distributed between 0.025 ppm to 0.043 ppm, since there are three WSs. Summarizing all the terms, the uncertainty for the estimated concentration ( $x$ ) is as follows:

$$U_x = \frac{1}{s} \cdot \sqrt{\frac{\sigma_y^2}{60} + \frac{1}{\sum w} + \frac{1}{s^2} \cdot \frac{(\sum wy - \sum wy)^2}{(\sum w)^2 (\sum wx^2) - (\sum wx)^2}} \quad (23-2)$$

Since the calculation was done for the logarithm of the concentration for CH<sub>4</sub>, the uncertainty for the estimated concentration was determined differently for the higher level ( $U^+ = x(e^{U_x} - 1)$ ) and lower level ( $U^- = x(1 - e^{-U_x})$ ). However, the average value is expressed as the uncertainty since the difference is less than 0.1 ppb in real terms.

削除:  $U^2$

削除:  $U^2$

削除:  $U^2$

削除: In most cases, the uncertainty for the concentration of standard gases is not given, or it can be negligible compared with other uncertainties. Thus, we neglected this term.

削除: →→→

書式を変更: フォント: Cambria Math

355 Figures S3 to S11 show the time series of uncertainty ( $U_{x\_sample}$ ) for the ambient air CO<sub>2</sub> concentration. Most uncertainties were distributed at 0.05 ppm but can be higher than 0.3 ppm, especially during summer. Note that the standard deviation of the output ( $\sigma_i$ ) of the sample air could become significant due to large diurnal variation during summer since the output of the sample air could include a natural variation of the atmosphere during the measurement period of three minutes. Figures S12 to S17 show the time series of uncertainty ( $U_{x\_sample}$ ) for the ambient air CH<sub>4</sub> concentration. Most are within five ppb but can be above ten ppb during the summer months. This is also due to the influence of natural variation and possibly heterogeneous CH<sub>4</sub> emissions from wetlands.

書式を変更: 下付き

書式を変更: 下付き

削除: 

書式を変更: 下付き

360 2.4.3 Reproducibility check with the SWS-gas measurement

We calculated a calibration line only when the SWS-gas measurements closest to both sides of the sample measurements were normal. The normality of the SWS-gas measurement was assessed as follows. The same on-site compressed air was measured several times (for about a week) since the air was used as SWS-gas until its pressure dropped below 0.1 MPa. The on-site compressed air output value would vary smoothly if the system were stable. When the system temporarily became unstable the corresponding large changes of the analyzer output could not be corrected by the SWS to a sufficient degree. To identify such occasions, we first estimated the output of standard gases at the time of the target SWS-gas measurement by interpolating  $\Delta^B(t_i)$  and  $\Delta^E(t_j)$  based on the output value of the target SWS-gas itself (Section 2.4.1). Then, calculating a calibration line with the estimated output of standard gases, we obtained the concentration of the target SWS-gas. Second, we estimated the output value of the SWS-gas at the time of the target SWS-gas measurement by interpolating the outputs of the two adjacent SWS-gases. Then, we determined the concentration of the target SWS-gas in the same manner. If these estimated concentrations differed from each other by more than one ppm for CO<sub>2</sub> and ten ppb for CH<sub>4</sub>, we regarded the target SWS-gas data as abnormal. This assessment (referred to as “self-check-value (scv) for SWS-gases” in Figure 5) was done while the adjacent SWS-gas measurements were conducted for the same on-site compressed air.

375 We then checked the system's stability with the measurement of the SWS-gas. Interpolating the outputs of the SWS-gases adjacent to the standard gas measurements, we calculated the concentrations of the SWS-gas with the calibration line at the time of STD2, which was used to assess the coefficient of determination in Section 2.3. We regarded the estimated concentrations of the SWS-gas as independent; thus, we obtained 14 estimated concentrations if the measurements for the same SWS-gas continued for a week. We determined a threshold for the standard deviation ( $\sigma_{SWS}$ ; 1 ppm for CO<sub>2</sub>, 10 ppb for CH<sub>4</sub>) and the fluctuation range (3 ppm for CO<sub>2</sub> and 30 ppb for CH<sub>4</sub>) obtained from the estimated independent data set. All the data that exceeded the threshold were deleted.

削除: However, a gap would appear if the system temporarily became unstable. To detect any gap

削除: s

削除: 5

削除: 2

380 The standard deviation of the remaining stable data provides reproducibility of repeat measurements every 12 hours for a given period (often a week). From the point of this procedure, the SWS-gas is similar to the short-term 'target tank' or 'surveillance tank' mentioned in the GAW report (WMO, 2020). Regardless of the site or time of measurement,  $\sigma_{SWS}$  for CO<sub>2</sub> mostly was

削除: equates with

削除: 18

書式を変更: 蛍光ペン (なし)

below 0.2 ppm, and for CH<sub>4</sub> was below five ppb (Supplement Figs. S3-S17). On the other hand, the CO<sub>2</sub> (CH<sub>4</sub>) concentrations in these observations can fluctuate on the order of ppm (10 ppb), even during a few hours of daytime when the atmosphere is well mixed (Sawakawa et al., 2010, 2013). It is, therefore, considered to be adequate for observations carried out in the vicinity of strong emission and absorption sources, such as those in the Siberian interior. The GAW report states that the compatibility goal for CO<sub>2</sub> (CH<sub>4</sub>) in the Northern Hemisphere is 0.1 ppm (2 ppb), but this is a target for background sites such as coastal areas and does not need to be strictly adapted to an observation area such as this study.

The uncertainty obtained for each sample air concentration ( $U_{x\_sample}$ ) with equation 23-2 could be more considerable than the reproducibility ( $\sigma_{sws}$ ). GAW report (WMO, 2020) mentioned that both values should be reported, and  $U_{x\_sample}$  provides a quantitative indicator of the influence of nearby sources and can be used for data selection and weighting in applications such as inverse modeling. Following this guide, we showed  $U_{x\_sample}$  and  $\sigma_{sws}$  in our data set. A flow chart for the calculation method is shown in Fig. 5.

- 削除: As examples, NOY data are shown in
- 削除: 1
- 削除: 1
- 書式を変更: 蛍光ペン (なし)
- 書式を変更: フォントの色: 自動, 蛍光ペン (なし)
- 書式を変更: 蛍光ペン (なし)
- 削除: Note that the standard deviation of the output ( $\sigma_x$ ) of the sample air could become significant due to large diurnal variation during summer since the output of the sample air could include a natural variation of the atmosphere during the measurement period of three minutes. As a result, t
- 削除: 18

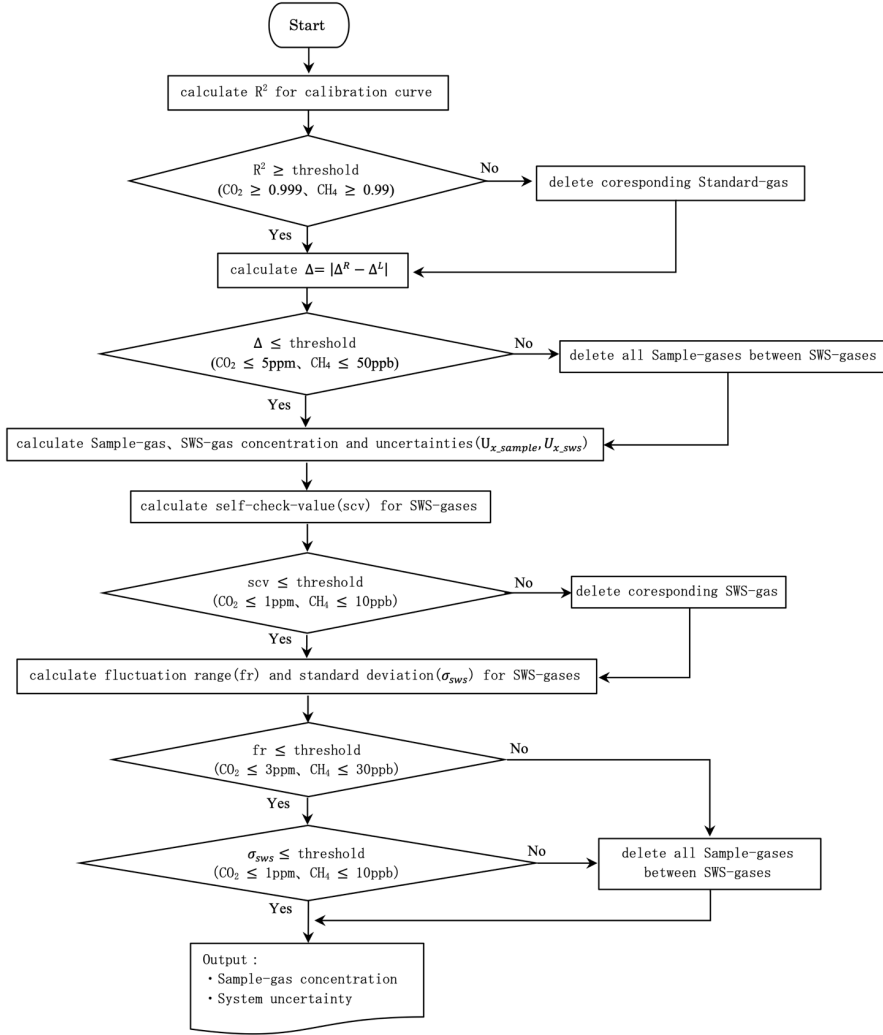
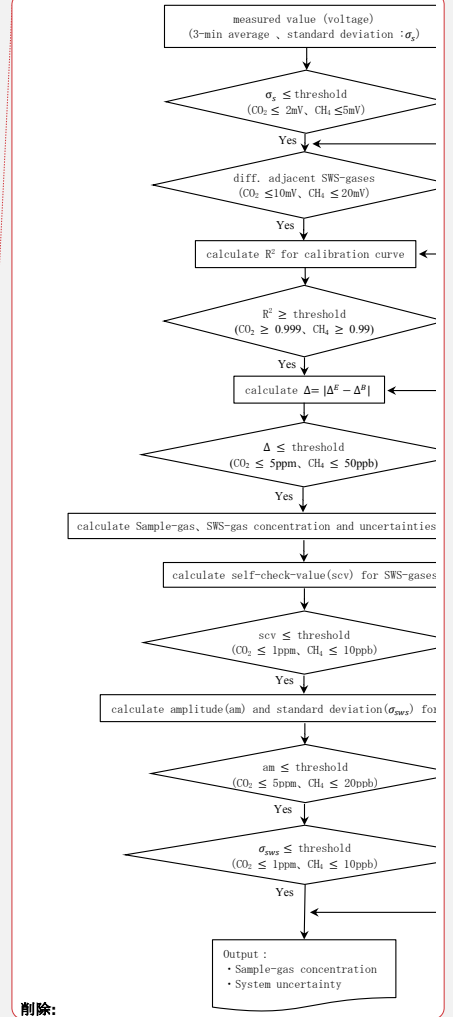


Figure 5. Flow chart of concentration calculation method.



2.5 Comparison between NDIR/TOS and CRDS

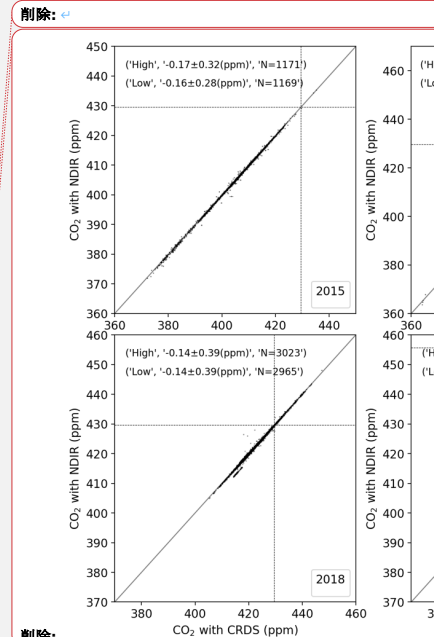
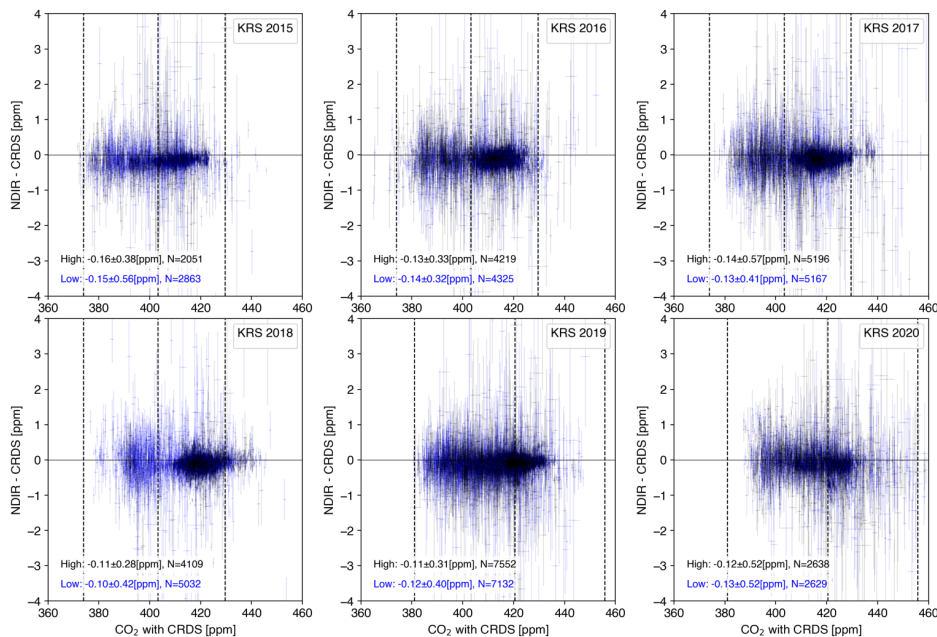
420 The CRDS operated at KRS from July 2015, DEM from June 2016, and NOY from August 2016, albeit for a short period of time for JR-STATION. The CRDS is a highly stable analyzer used in greenhouse gas observations worldwide (Kwok et al., 2015). We compared the recalculated NDIR (and TOS) values with the CRDS values (Fig. 6, Fig. 7, Supplement Fig. S18-S21). The flow path branches off after the 6-port valve (Fig. 1), so the same air is analyzed. The CRDS operates independently of the existing system, so information on instrument error flags and valve switching timing is not linked to the measured data. Therefore, by detecting the CH<sub>4</sub> concentration of the lowest standard gas, the timing of the standard gas measurement was captured and timed. Only data from periods was extracted when the SWS results fulfilled the criteria outlined in the previous section. The CRDS output values were converted to the NIES scale based on the WS measurements and averaged over three minutes for comparison. The temperature in the warm box of CRDS (data column name is ‘WarmBoxTemperature’) was kept constant (45.00°C). Still, it rarely changed by more than 0.03°C in 3 minutes, and the data was not used for comparison as the system was not considered stable during these periods. Since some observed values exceeded the highest concentration of the standard gas, only values within the concentration range of the standard gas were used to calculate the difference between the two. There was no significant difference in CO<sub>2</sub> concentration regardless of the inlet at both altitudes (Fig. 6, Supplement Figs. S18-S20). As stated in Section 2.4.2, natural variability within the measurement time (3 minutes) caused a more significant error bar during summer (Supplement Fig. S20). No significant difference was found for CH<sub>4</sub> concentration either at KRS (Fig. 7). At NOY and DEM, it was discovered that the temperature controller of the catalytic unit was not functioning correctly. Since the TOS is sensitive to CO and H<sub>2</sub> in the air, it could produce unusually high values without a proper catalytic unit. For the period, only the data from the CRDS should be published. Since no catalytic unit errors were identified at the other sites, the ambient atmospheric values were detected, as is the case with KRS.

- 削除: was install
- 削除: in
- 削除: in
- 削除: in
- 削除: semiconductor sensor
- 削除: 7
- 書式を変更: 蛍光ペン (なし)
- 削除: 10
- 削除: Only data from the period when the system was normal was extracted.

- 削除: 2
- 削除: in DEM and NOY,
- 削除: and the CO<sub>2</sub> concentration fluctuated more in such cases
- 削除: The CH<sub>4</sub> concentration, on the other hand, was not affected by this temperature change.

- 削除: However, the difference in NOY was highly variable, and the TOS values tended to be significantly higher. The sensor is also sensitive to CO and H<sub>2</sub> in the air, so these gases are removed by installing a catalyst just before the sensor. However, it was found that the catalyst had deteriorated, and a new catalytic unit had to be added. The sensitivity of CO and H<sub>2</sub> to the semiconductor sensor is reported to be about 10% of that by CH<sub>4</sub> (Suto and Inoue, 2010), but if CO (about 100 ppb) and H<sub>2</sub> (about 500 ppb) are not removed at all from the air, an excess of about 60 ppb as CH<sub>4</sub> concentration could be detected. In NOY, it is expected that the temperature regulation of the catalytic unit did not work well and the catalyst did not function; only the CRDS measurements of the CH<sub>4</sub> concentration in NOY shall be used.<sup>4)</sup>





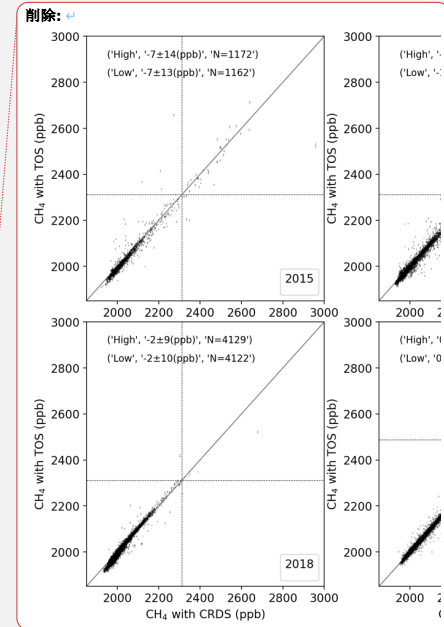
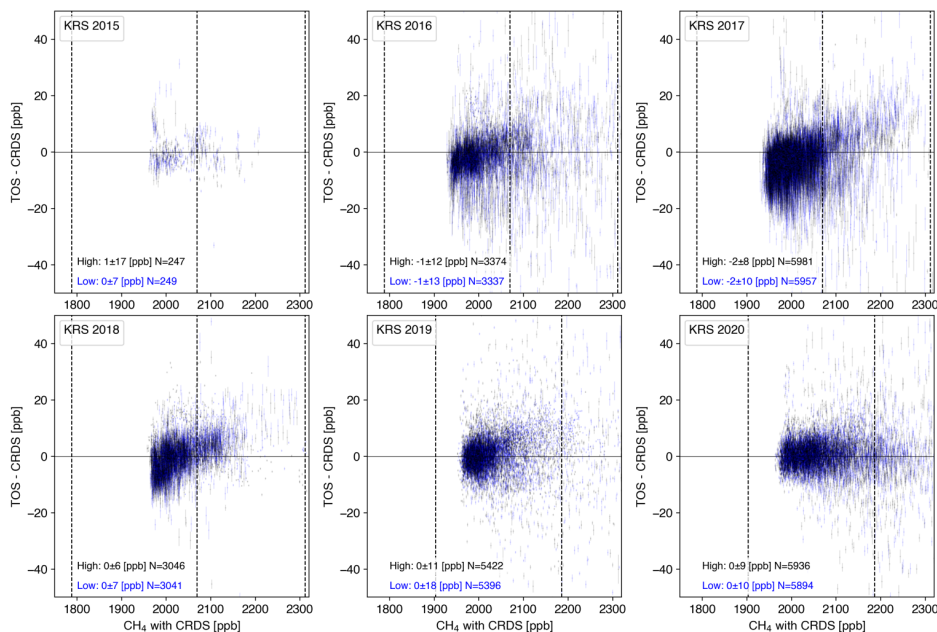
削除: 書式を変更: 下付き

削除: Relationship between CO<sub>2</sub> concentration measured by the NDIR and the CRDS during ambient air measurements at KRS. The CRDS 3-minute measurements are averaged on the horizontal axis, and the NDIR values are on the vertical axis. Error bars on the horizontal axis are the standard error of the averaged data. Error bars on the vertical axis are  $U_{x\_sample}$ . The gray line represents the 1:1 line.

削除: highest

削除: between NDIR and CRDS (NDIR - CRDS)

書式を変更: 英語 (米国)



削除: Relationship between  $\text{CH}_4$  concentration measured by the TOS and the CRDS during ambient air measurements at KRS. The CRDS 3-minute measurements are averaged on the horizontal axis, and the TOS values are on the vertical axis. Error bars on the horizontal axis are the standard deviation of the averaged data. Error bars on the vertical axis are  $U_{\text{sample}}$ . The gray line represents the 1:1 line.

削除: highest

削除: between TOS and CRDS ( $\text{TOS} - \text{CRDS}$ )

書式を変更: 取り消し線

#### Data availability

The data are available from the Global Environmental Database, hosted by GED, CGER, NIES (<http://db.cger.nies.go.jp/portal/geds/index>).

**Author contribution**

MS and NT designed the study. MS wrote the manuscript. MA, DD, and AF conducted the measurements. All authors contributed to the discussion and preparation of the manuscript.

**Competing interests**

The authors declare that they have no conflict of interest.

**Acknowledgments**

We thank Sergey Mitin (Institute of Microbiology, Russian Academy of Sciences) for administrative support. Our research was financially supported by the Global Environmental Research Coordination System from Ministry of the Environment of Japan (E0752, E1254, E1752, E2251) and the most important innovative project of national importance "Development of a system for ground-based and remote monitoring of carbon pools and greenhouse gas fluxes in the territory of the Russian Federation, ensuring the creation of recording data systems on the fluxes of climate-active substances and the carbon budget in forests and other terrestrial ecological systems" (Registration number: 123030300031-6).

**References**

Andrews, A. E., Kofler, J. D., Trudeau, M. E., Williams, J. C., Neff, D. H., Masarie, K. A., Chao, D. Y., Kitzis, D. R., Novelli, P. C., Zhao, C. L., Dlugokencky, E. J., Lang, P. M., Crotwell, M. J., Fischer, M. L., Parker, M. J., Lee, J. T., Baumann, D. D., Desai, A. R., Stanier, C. O., De Wekker, S. F. J., Wolfe, D. E., Munger, J. W., and Tans, P. P.: CO<sub>2</sub>, CO, and CH<sub>4</sub> measurements from tall towers in the NOAA Earth System Research Laboratory's Global Greenhouse Gas Reference Network: instrumentation, uncertainty analysis, and recommendations for future high-accuracy greenhouse gas monitoring efforts, Atmospheric Measurement Techniques, 7, 647-687, 10.5194/amt-7-647-2014, 2014.

ICOS RI: ICOS Atmosphere Station Specifications V2.0, edited by: Laurent, O., ICOS ERIC, <https://doi.org/10.18160/GK28-2188>, 2020.

Kwok, C. Y., Laurent, O., Guemri, A., Philippon, C., Wastine, B., Rella, C. W., Vuillemin, C., Truong, F., Delmotte, M., Kazan, V., Darding, M., Lebegue, B., Kaiser, C., Xueref-Remy, I., and Ramonet, M.: Comprehensive laboratory and field testing of cavity ring-down spectroscopy analyzers measuring H<sub>2</sub>O, CO<sub>2</sub>, CH<sub>4</sub> and CO, Atmospheric Measurement Techniques, 8, 3867-3892, 10.5194/amt-8-3867-2015, 2015.

Machida, T., Tohjima, Y., Katsumata, K. and Mukai, H.: A new CO<sub>2</sub> calibration scale based on gravimetric one-step dilution cylinders in National Institute for Environmental Studies – NIES 09 CO<sub>2</sub> Scale, in Report of the 15th WMO/IAEA Meeting of

削除: <https://doi.org/10.18160/GK28-2188>

書式を変更: 段落フォント, 英語 (英国)

Experts on Carbon Dioxide, Other Greenhouse Gases and Related Tracers Measurement Techniques (ed. Willi A. Brand). Jena, Germany, September 7–10, 2009, WMO/GAW Report No. 194, 165–169, 2011.

Sasakawa, M., Machida, T., Tsuda, N., Arshinov, M., Davydov, D., Fofonov, A., and Krasnov, O.: Aircraft and tower measurements of CO<sub>2</sub> concentration in the planetary boundary layer and the lower free troposphere over southern taiga in West Siberia: Long-term records from 2002 to 2011, *Journal of Geophysical Research-Atmospheres*, 118, 9489-9498, 10.1002/jgrd.50755, 2013.

Sasakawa, M., Ito, A., Machida, T., Tsuda, N., Niwa, Y., Davydov, D., Fofonov, A., and Arshinov, M.: Annual variation of CH<sub>4</sub> emissions from the middle taiga in West Siberian Lowland (2005-2009): a case of high CH<sub>4</sub> flux and precipitation rate in the summer of 2007, *Tellus Series B-Chemical and Physical Meteorology*, 64, ARTN 17514 10.3402/tellusb.v64i0.17514, 2012.

Sasakawa, M., Shimoyama, K., Machida, T., Tsuda, N., Suto, H., Arshinov, M., Davydov, D., Fofonov, A., Krasnov, O., Saeki, T., Koyama, Y., and Maksyutov, S.: Continuous measurements of methane from a tower network over Siberia, *Tellus Series B-Chemical and Physical Meteorology*, 62, 403-416, 10.1111/j.1600-0889.2010.00494.x, 2010.

Schibig, M. F., Kitzis, D., and Tans, P. P.: Experiments with CO<sub>2</sub>-in-air reference gases in high-pressure aluminum cylinders, Atmospheric Measurement Techniques, 11, 5565-5586, 10.5194/amt-11-5565-2018, 2018.

Suto, H. and Inoue, G.: A New Portable Instrument for In Situ Measurement of Atmospheric Methane Mole Fraction by Applying an Improved Tin Dioxide-Based Gas Sensor, *J Atmos Ocean Tech*, 27, 1175-1184, 10.1175/2010jtecha1400.1, 2010.

Tohjima, Y., Machida, T., Mukai, H., Maruyama, M., Nishino, T., Akama, I., Amari, T., and Watai, T.: Preparation of gravimetric CO<sub>2</sub> standards by one-step dilution method, In: John B. Miller eds. 13th IAEA/WMO Meeting of CO<sub>2</sub> Experts, Vol WMO-GAW Report 168. Boulder, 2005, 26-32, 2006.

Tohjima, Y., Katsumata, K., Morino, I., Mukai, H., Machida, T., Akama, I., Amari, T., and Tsunogai, U.: Theoretical and experimental evaluation of the isotope effect of NDIR analyzer on atmospheric CO<sub>2</sub> measurement, J. Geophys. Res., 114, 10.1029/2009JD011734, 2009.

Watai, T., Machida, T., Shimoyama, K., Krasnov, O., Yamamoto, M., and Inoue, G.: Development of an Atmospheric Carbon Dioxide Standard Gas Saving System and Its Application to a Measurement at a Site in the West Siberian Forest, *J Atmos Ocean Tech*, 27, 843-855, 10.1175/2009jtecha1265.1, 2010.

Winderlich, J., Chen, H., Gerbig, C., Seifert, T., Kolle, O., Lavric, J. V., Kaiser, C., Hoefler, A., and Heimann, M.: Continuous low-maintenance CO<sub>2</sub>/CH<sub>4</sub>/H<sub>2</sub>O measurements at the Zotino Tall Tower Observatory (ZOTTO) in Central Siberia, Atmospheric Measurement Techniques, 3, 1113-1128, 10.5194/amt-3-1113-2010, 2010.

WMO: 20th WMO/IAEA Meeting on Carbon Dioxide, Other Greenhouse Gases and Related Measurement Techniques (GGMT-2019), Jeju Island, South Korea, 2–5 September, 2019, GAW Report No. 255, World Meteorological Organization, Geneva, Switzerland, 2020.

書式を変更: 下付き

書式を変更: 下付き

削除: 19

削除: Tracers

削除: -

削除: 7

削除: Dübendorf, Switzerland

削除: 7

削除: 31

削除: August

削除: 7

削除: 42

削除: -

削除: 18

削除: ↩

↩